Herrmann, R., Neugebauer, K., Pirkl, E., Zentgraf, H., & Schaller, H. (1980) *MGG, Mol. Gen. Genet. 177*, 231–242.
Hotta, Y., & Stern, H. (1978) *Biochemistry 17*, 1872–1880.
Hyodo, M., & Suzuki, K. (1981) *Cell Struct. Funct. 6*, 35–42.
Kawasaki, K., Nagata, K., Enomoto, T., Hanaoka, F., & Yamada, M. (1982) *Biochem. Int. 5*, 121–128.
Kawasaki, K., Nagata, K., Enomoto, T., Hanaoka, F., & Yamada, M. (1984) *J. Biochem. (Tokyo) 95*, 485–493.
Korn, L. J., & Yanofsky, C. (1976) *J. Mol. Biol. 106*, 231–241.
Mace, D. C., & Alberts, B. M. (1984) *J. Mol. Biol. 177*, 279–293.
Maniatis, T., Fritsch, E. F., & Sambrook, J. (1982) *Molecular Cloning*, pp 90–94, Cold Spring Harbor Laboratory, New York.
Menetski, J. P., & Kowalczykowski, S. C. (1985) *J. Mol. Biol. 181*, 281–295.
Murakami, Y., Yasuda, H., Miyazawa, H., Hanaoka, F., & Yamada, M. (1985) *Proc. Natl. Acad. Sci. U.S.A. 82*, 1761–1765.
Nakano, M. M., Sekiguchi, T., & Yamada, M. (1978) *Somatic Cell Genet. 4*, 169–178.
Nishimura, M., Yasuda, H., Ikegami, S., Ohashi, M., & Yamada, M. (1979) *Biochem. Biophys. Res. Commun. 91*, 939–945.
Otto, B. (1977) *FEBS Lett. 79*, 175–178.
Plevani, P., Badaracco, G., & Chang, L. M. S. (1980) *J. Biol. Chem. 255*, 4957–4963.
Shibata, T., DasGupta, C., Cunningham, R. P., & Radding, C. M. (1979) *Proc. Natl. Acad. Sci. U.S.A. 76*, 1638–1642.
Suzuki, M., Enomoto, T., Hanaoka, F., & Yamada, M. (1985) *J. Biochem. (Tokyo) 98*, 581–584.
Tanuma, S., Enomoto, T., & Yamada, M. (1980) *Cell Struct. Funct. 5*, 27–37.
Tawaragi, Y., Enomoto, T., Watanabe, Y., Hanaoka, F., & Yamada, M. (1984) *Biochemistry 23*, 529–533.
Thomas, D. C., & Meyer, R. R. (1982) *Biochemistry 21*, 5060–5068.
Tsai, Y.-J., Hanaoka, F., Nakano, M. M., & Yamada, M. (1979) *Biochem. Biophys. Res. Commun. 91*, 1190–1195.
Watanabe, Y., Tawaragi, Y., Enomoto, T., Hanaoka, F., & Yamada, M. (1981) *Biochem. Int. 3*, 407–413.
Watanabe, Y., Nagata, K., Tawaragi, Y., Enomoto, T., Hanaoka, F., & Yamada, M. (1982) *FEBS Lett. 149*, 44–46.
Weinstock, G. M., McEntee, K., & Lehman, I. R. (1979) *Proc. Natl. Acad. Sci. U.S.A. 76*, 126–130.
Yaginuma, K., & Koike, K. (1981) *Nucleic Acids Res. 9*, 1949–1961.
Yasuda, H., Matsumoto, Y., Mita, S., Marunouchi, T., & Yamada, M. (1981) *Biochemistry 20*, 4414–4419.

Affinities of tRNA Binding Sites of Ribosomes from *Escherichia coli*†

Roland Lill, James M. Robertson, and Wolfgang Wintermeyer*
Institut für Physiologische Chemie, Physikalische Biochemie, und Zellbiologie der Ludwig-Maximilians-Universität München, D-8000 München 2, Federal Republic of Germany

Received October 3, 1985; Revised Manuscript Received January 30, 1986

ABSTRACT: The binding affinities of $tRNA^{Phe}$, Phe-$tRNA^{Phe}$, and *N*-AcPhe-$tRNA^{Phe}$ from either *Escherichia coli* or yeast to the P, A, and E sites of *E. coli* 70S ribosomes were determined at various ionic conditions. For the titrations, both equilibrium (fluorescence) and nonequilibrium (filtration) techniques were used. Site-specific rather than stoichiometric binding constants were determined by taking advantage of the varying affinities, stabilities, and specificities of the three binding sites. The P site of poly(U)-programmed ribosomes binds $tRNA^{Phe}$ and *N*-AcPhe-$tRNA^{Phe}$ with binding constants in the range of 10^8 M^{-1} and 5×10^9 M^{-1}, respectively. Binding to the A site is 10–200 times weaker, depending on the Mg^{2+} concentration. Phe-$tRNA^{Phe}$ binds to the A site with a similar affinity. Coupling A site binding of Phe-$tRNA^{Phe}$ to GTP hydrolysis, by the addition of elongation factor Tu and GTP, leads to an apparent increase of the equilibrium constant by at least a factor of 10^4. Upon omission of poly(U), the affinity of the P site is lowered by 2–4 orders of magnitude, depending on the ionic conditions, while A site binding is not detectable anymore. The affinity of the E site, which specifically binds deacylated $tRNA^{Phe}$, is comparable to that of the A site. In contrast to P and A sites, binding to the E site is labile and insensitive to changes of the ionic strength. Omission of the mRNA lowers the affinity at most by a factor of 4, suggesting that there is no efficient codon–anticodon interaction in the E site. On the basis of the equilibrium constants, the displacement step of translocation, to be exergonic, requires that the tRNA leaving the P site is bound to the E site. Under in vivo conditions, the functional role of transient binding of the leaving tRNA to the E site, or a related site, most likely is to enhance the rate of translocation.

Understanding the mechanism of protein biosynthesis on a molecular level requires—in addition to biochemical, structural, and kinetic information—the knowledge of the thermodynamic parameters of the individual steps of the process. Most important in that respect are the interactions between tRNA and its ribosomal binding sites. For charged tRNA, the ribosome possesses two of them, to which aminoacyl-tRNA (A site) and peptidyl-tRNA (P site) are bound in the state before peptide bond formation. An additional site (E site), which is accessible for deacylated tRNA only, was found for eucaryotic ribosomes (Wettstein & Noll, 1965) and has recently been shown to exist also on *Escherichia coli*

† This work was supported by the Deutsche Forschungsgemeinschaft and the Fonds der Chemischen Industrie. W.W. acknowledges a Heisenberg fellowship from the Deutsche Forschungsgemeinschaft.

0006-2960/86/0425-3245$01.50/0

ribosomes (Rheinberger et al., 1981; Grajevskaja et al., 1982; Kirillov et al., 1983; Lill et al., 1984). For this site, an exit function has been postulated in the sense that during translocation deacylated tRNA is transported from the P to the E site before leaving the ribosome (Noll, 1966; Rheinberger & Nierhaus, 1983).

Binding affinities for the interaction of tRNA with the ribosomal sites, mostly the P and A sites, have been determined by a number of groups. Unfortunately, the published data are difficult to use, since they vary up to 100-fold. For instance, the affinity of the P site for the peptidyl-tRNA analogue *N*-AcPhe-tRNA^{Phe} has been reported to be about 5×10^8 M^{-1} (Kirillov & Semenkov, 1982) or about 4×10^6 M^{-1} (Rheinberger et al., 1981; Schmitt et al., 1982). Similarly, the values reported for binding *N*-AcPhe-tRNA^{Phe} to the A site range from 2×10^7 M^{-1} (Kirillov & Semenkov, 1982) and 3×10^6 M^{-1} (Rheinberger et al., 1981) to 2×10^5 M^{-1} (Schmitt et al., 1982). Substantially divergent data have also been reported for the binding of deacylated tRNA to its ribosomal binding sites (Fairclough et al., 1979; Peters & Yarus, 1979; Rheinberger et al., 1981; Kirillov et al., 1983).

Different experimental conditions such as Mg^{2+} concentration, ionic strength, and temperature cannot explain the considerable variations of the published binding constants. Rather, the differences in the tRNA binding capacity of the ribosomes, in the experimental techniques, and in the evaluation of the titration data may have led to different results. Furthermore, the earlier reports did not take into account the binding of deacylated tRNA^{Phe} to the E site (Fairclough et al., 1979; Peters & Yarus, 1979), although even data that were evaluated on the basis of three binding sites for uncharged tRNA differ considerably, especially for tRNA binding to the P site (Rheinberger et al., 1981; Kirillov et al., 1983).

The experimental technique used to determine the extent of tRNA–ribosome complex formation appears to be particularly important, at least for studying rapidly dissociating complexes. In most of the previous reports, the amount of ribosome-bound tRNA was determined by the nitrocellulose filtration technique, which, as a nonequilibrium method, is limited to the detection of rather stable complexes. Equilibrium methods allowing also the detection of rapidly dissociating complexes, such as fluorescence (Fairclough et al., 1979) or ultracentrifugation (Schmitt et al., 1982), have been employed in only a few studies. In the present study, three different techniques have been used for the determination of ribosome-bound tRNA: (i) nitrocellulose filtration with radioactively labeled tRNAs, (ii) an indirect indicator binding assay, in which the extent of complex formation was followed by the inhibition of binding of small amounts of an indicator tRNA added in a subsequent step (Lill et al., 1984), and (iii) fluorescence measurements utilizing fluorescent tRNA derivatives. Fluorescent reporter groups were the natural fluorophor wybutine in the anticodon loop of yeast tRNA^{Phe} and proflavin replacing dihydrouracil in the D loop of tRNA^{Phe} from yeast (Wintermeyer & Zachau, 1979) and *E. coli* (W. Wintermeyer, unpublished results).

Using these techniques, we have determined the affinities of the P, A, and E sites of 70S tight-couple ribosomes from *E. coli* for tRNA^{Phe}, Phe-tRNA^{Phe}, and *N*-AcPhe-tRNA^{Phe}. The tRNA binding activity of the ribosomes was characterized by indicator titrations, as described previously (Lill et al., 1984). Binding constants have been measured at different conditions with respect to Mg^{2+} concentration and ionic strength. In addition, the influence of the presence or absence of poly(U) and of elongation factor Tu–GTP upon the binding strength has been studied. In order to obtain site-specific binding constants, particular attention was given to the problem created by the availability of two or three ribosomal tRNA binding sites exhibiting either very different (P and A sites) or rather similar (A and E sites) affinities.

Materials and Methods

Materials

Ribosomes, tRNA, and Elongation Factor Tu. The preparation of tight-couple 70S ribosomes from *E. coli* MRE 600 was described in a previous publication (Robertson & Wintermeyer, 1981). Ribosome concentrations are given as the fraction of ribosomes active in binding tRNA^{Phe} or *N*-Ac-Phe-tRNA^{Phe} to both P and A sites as determined by the indicator titrations described earlier (Lill et al., 1984). Relative to the conversion factor of 23 pmol/A_{260} unit, the activity of several ribosome preparations used ranged from 60 to 80%.

tRNA^{Phe} from *E. coli* (charging capacity 1.3–1.5 nmol of Phe/A_{260} unit) was purchased from Boehringer, Mannheim. The isolation of tRNA^{Phe} (1.5–1.7 nmol of Phe/A_{260} unit) from brewers' yeast tRNA (Boehringer, Mannheim), as well as the aminoacylation and acetylation of the tRNA^{Phe}s, was described previously (Robertson & Wintermeyer, 1981; Lill et al., 1984). [^{14}C]Phe-tRNA^{Phe} and *N*-Ac[^{14}C]Phe-tRNA^{Phe} (504 Ci/mol, if not stated otherwise) were charged to 70–80% and 80–95%, respectively, 100% being 1.8 nmol/A_{260} unit (Guêron & Leroy, 1978). For nonenzymatic titrations, [^{14}C]Phe-tRNA^{Phe} was prepared by incubation (30 min at 37 °C) with purified phenylalanyl-tRNA ligase from yeast (1.5 milliunits/mL; Hirsch & Zachau, 1976) in the respective titration buffer containing up to 5 μM tRNA^{Phe}, 50 μM L-[^{14}C]phenylalanine, 3 mM ATP, 0.3 mM GTP, 6 mM phosphoenolpyruvate, and pyruvate kinase (10 μg/mL) and used without isolation ("in situ" aminoacylation).

The radioactive label in [^{32}P]tRNA^{Phe} was introduced by enzymatic exchange of the 5′-phosphate with alkaline phosphatase and polynucleotide kinase (Lill et al., 1984). Fluorescent tRNA$^{Phe}_{Prfl6/17}$ from yeast (charging capacity 1.2–1.5 nmol of Phe/A_{260} unit) carrying proflavin instead of dihydrouracil in position 16 or 17 was prepared according to Wintermeyer and Zachau (1979). Proflavin-labeled tRNA^{Phe} from *E. coli*, tRNA$^{Phe}_{Prfl6/20}$ (charging capacity about 1.3 nmol of Phe/A_{260} unit), was prepared by the same procedure; details will be published elsewhere.

Elongation factor Tu (EF-Tu) from *E. coli* MRE 600 was isolated according to a published procedure (Leberman et al., 1980), except that cells were opened by alumina grinding and 10 μM GDP was present throughout the preparation. The protein was further purified by crystallization (Chinali et al., 1977) and appeared at least 99.5% pure according to sodium dodecyl sulfate (SDS)–polyacrylamide gel electrophoresis. The formation of the ternary complex Phe-tRNA^{Phe}·EF-Tu·GTP has been detailed earlier (Lill et al., 1984).

Buffers. The following buffers were used: (A) 50 mM tris(hydroxymethyl)aminomethane hydrochloride (Tris-HCl), pH 7.5, 50 mM KCl, 90 mM NH_4Cl, 1 mM dithioerythritol, and 20 or 10 mM magnesium acetate, as indicated; (B) mM Tris-HCl, pH 7.5, 30 mM KCl, 30 mM NH_4Cl, 1 mM dithioerythritol, and 15, 10, or 6 mM magnesium acetate, as indicated; (C) 10 mM Tris-HCl, pH 7.5, 35 mM NH_4Cl, 1 mM dithioerythritol, and 20 mM magnesium acetate.

Equilibrium Titrations

Three different methods were applied for the determination of binding constants. Two of these, the nitrocellulose filtration technique and the indicator titration assay, have been described

earlier (Lill et al., 1984). In addition, fluorescence titrations were performed, in which the binding of fluorescent tRNAs to ribosomes was monitored by an increase of the fluorescence intensity (Robertson et al., 1977).

In general, titrations were carried out at 20 °C in separate incubation mixtures by varying the amount of labeled tRNA at a constant ribosome concentration; the latter normally was kept in the range of the dissociation constant of the examined binding site. Poly(U) was present in a concentration of 1 A_{260} unit/mL, if not stated otherwise. For blocking either the P site alone or both P and A sites (Lill et al., 1984) during the titrations of the A or E site, ribosomes (about 0.5 μM) were preincubated with a 1.1- or 2.3-fold excess of either deacylated $tRNA^{Phe}$ or *N*-AcPhe-$tRNA^{Phe}$. The errors of the binding constants due to the slight excess of blocking tRNA are estimated to be below 10%. In order to account for the slowness of nonenzymatic binding to the A site (see Results), the reaction mixtures (except those described below) were incubated for 30, 60, 90, or 120 min at 20, 15, 10, or 6 mM Mg^{2+} concentration, respectively, before being further analyzed for the extent of complex formation. During nonenzymatic titrations with Phe-$tRNA^{Phe}$, the charging level was kept higher than 1.2 nmol of Phe/A_{260} unit by the use of in situ aminoacylated Phe-$tRNA^{Phe}$, as described above. In filtration experiments, the blank values generally did not exceed 2% of the total signal and were subtracted. In order to reach such low blank values during titrations with in situ aminoacylated Phe-$tRNA^{Phe}$, the nitrocellulose filters were washed with buffer containing 5 mM unlabeled phenylalanine.

In titrations where tRNA–ribosome complex formation was rather fast, i.e., during the titrations of the E site, in the absence of mRNA, or in the presence of EF-Tu, the reaction mixtures were incubated for about 1 min after the addition of the tRNA. During the fluorescence titrations (see below), an alternative procedure, which allowed the addition of fluorescent tRNA by steps, proved to be more accurate and material saving. tRNA was added in small portions to the cuvette containing buffer and poly(U), if indicated, by means of a 50-μL syringe with dispenser (PB-600, Hamilton Bonaduz). After a correction for dilution (less than 12% after all additions), fluorescence data were further processed as described below.

Fluorescence was measured with a photon-counting spectrofluorometer equipped with a 450-W xenon lamp (Osram) and double monochromators for excitation (Schoeffel GM 252 D) and emission (Schoeffel GM 200). The fluorescence signal was measured relative to the intensity of the exciting light by means of two photomultipliers (RCA 8850) and a two-channel single-photon counter (Ortec-Brookdeal, 5C1) and transferred to a microcomputer (Tektronix 4052) for data evaluation. Excitation wavelengths for the wybutine and proflavin fluorophores were 317 and 442 nm; emission was monitored at 425 and 492 nm, respectively.

Fluorescence titration data were obtained from the difference of the signals in the presence ("complex titration") and the absence ("reference titration") of ribosomes. Scatter was minimized by the subtraction of reference data points corrected by linear regression of the total reference curve rather than the individually measured data points. Titrations were usually performed at concentrations high enough to keep the signal/noise ratio greater than 50 at the final titration plateau.

Evaluation of Equilibrium Titration Data

As mentioned in the introduction, *E. coli* ribosomes possess three binding sites for deacylated $tRNA^{Phe}$ (P, A, and E sites), two of which (P and A sites) are also accessible for charged tRNA. The availability of three or two binding sites complicates the determination of binding constants, since in the absence of additional information, only stoichiometric rather than site-specific binding constants can be obtained (Klotz, 1974). For the present problem, the biochemical information regarding the sequence and stability of tRNA binding to the ribosomal sites was used to simplify the "three- or two-site" problem by converting it into three or two "single-site" problems. In the following, this approach, which allows the determination of site-specific binding constants, is first exemplified in a general way; then, the formal treatment of the various models ("single-site", "two-site", and "three-site" models) used for data evaluation is presented.

Regardless of whether charged or uncharged $tRNA^{Phe}$ is added to poly(U)-programmed, vacant ribosomes, the P site is the first site to be occupied (Watanabe, 1972; Lill et al., 1984). With charged $tRNA^{Phe}$, the second site to be occupied is the A site. Thus, in the general scheme (eq 1a) for the

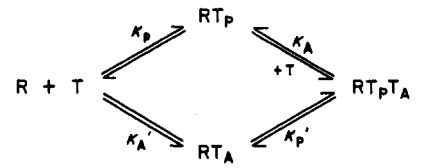

(1a)

binding of charged $tRNA^{Phe}$, T, to two different sites, P and A, on poly(U)-programmed ribosomes, R, the lower branch, representing tRNA binding to the A site of vacant ribosomes, can be neglected (i.e., $K_A' \ll K_P$). The sequential binding of charged $tRNA^{Phe}$ to P and A sites can be understood on the basis of the affinities of the two sites, which differ by at least a factor of 20 under all conditions tested (see Results). It is to be noted, though, that the observed preference for the P site is even more pronounced than predicted by the affinity difference. This is due to kinetic reasons. tRNA binding to the P site is about 100 times faster than to the A site (Wintermeyer & Robertson, 1982), while the dissociation from both sites is very slow (hours; see Results). Thus, within the time span of a titration experiment, about 0.5 h, the distribution of the tRNAs between the two sites will be determined by the binding rates rather than by the affinities. As a consequence, the two sites are occupied sequentially with a 100-fold preference of the P site over the A site.

The "nonequilibrium" distribution of the tRNAs with respect to the relative occupancy of the A site is implicated in the binding model used below for the evaluation of the titration data. The model assumes that significant amounts of tRNA become available for binding to the A site only after equilibration of the P site. On the other hand, when the P site is blocked, the A site may be titrated independently of the P site (single-site model). In turn, the A site binding constant may be used as a known parameter when evaluating the simultaneous titration of both P and A sites with charged $tRNA^{Phe}$ (two-site model).

A sequential binding model is valid also for the distribution of deacylated $tRNA^{Phe}$ between the P, A, and E sites. As mentioned above, deacylated tRNA will bind to the P site first. The sequence of binding to the remaining two sites depends upon the tRNA used. While with $tRNA^{Phe}$ from *E. coli* the E site is occupied prior to or concomitantly with the A site, in the case of $tRNA^{Phe}$ from yeast the A site is occupied prior to the E site (Lill et al., 1984). In addition, A and E sites appear to be occupied independently of each other, as indicated by the observation that occupancy of the A site does not induce tRNA release from the E site (Wintermeyer et al., 1986). Thus, by use of ribosomes whose P and A sites are preoccupied

either with deacylated $tRNA^{Phe}$ from yeast or with N-Ac-Phe-$tRNA^{Phe}$, the titration of the E site with $tRNA^{Phe}$ reduces to a single-site problem. The binding constant of the E site, in turn, may be used in evaluating an A site binding constant of deacylated $tRNA^{Phe}$ from yeast (two-site model). Finally, both binding constants are required to evaluate a P-site titration (three-site model).

Single-Site Model. At high ribosome concentrations, which are necessary for the titration of the weaker A site, it is possible to block the P site specifically with stoichiometric amounts of $tRNA^{Phe}$ (Lill et al., 1984). Therefore, as discussed above, the evaluation of the A site titration can be accomplished separately by the use of a single-site model. This is depicted in eq 2a, where t and T denote unlabeled blocking tRNA and

$$R + t \underset{K_P}{\rightleftharpoons} Rt_P \overset{+T}{\underset{K_A}{\rightleftharpoons}} Rt_PT_A \qquad (2a)$$

radioactively or fluorescence labeled tRNA, respectively. (An analogous formalism applies for E site titrations after blocking both P and A sites with, e.g., *N*-AcPhe-$tRNA^{Phe}$.) The fractional saturation of the A site n_A at a given tRNA concentration, c_{T^0}, can be derived from the law of mass action (Winkler-Oswatitsch & Eigen, 1979) and is expressed in eq 3a.

$$n_A(c_{T^0}) = [L - (L^2 - 4c_{T^0}c_{R^0})^{1/2}]/(2c_{R^0}) \qquad (3a)$$

$$L = c_{T^0} + c_{R^0} + 1/K_A$$

c_{T^0} and c_{R^0} = total concentrations of T and R

n_A is related to the amount of bound tRNA I_A according to

$$I_A(c_{T^0}) = I_{max}n_A(c_{T^0}) + I_B \qquad (4a)$$

I_B and $I_{max} + I_B$ denote the signals observed without tRNA added and at saturation, respectively. Equation 4a served to estimate the binding constant K_A by a Gauss–Newton iteration procedure (Graybill, 1969). Optimal fits are obtained when the parameters I_{max} and I_B are also fitted. Typically, the errors of the parameters due to data scatter are below 10%.

Two-Site Model. For titrations in which subsequently to the P site also the A site is occupied, the total amount of ribosome-bound tRNA (relative to total ribosomes, c_{R^0}) is given by the sum of the fractional saturations of the two sites $n_P + n_A$. If the sequential binding model depicted in eq 2a is assumed, n_P can be expressed analogously to the single-site model (cf. eq 3a):

$$n_P(c_{T^0}) = [M - (M^2 - 4c_{T^0}c_{R^0})^{1/2}]/(2c_{R^0}) \qquad (3b)$$

$$M = c_{T^0} + c_{R^0} + 1/K_P$$

For the calculation of n_A, the remaining concentration of tRNA available for binding to the A site c_{TA} follows from the difference of the total concentration of tRNA c_{T^0} and the amount bound to the P site (eq 5a). Then, the fractional

$$c_{TA}(c_{T^0}) = c_{T^0} - n_P(c_{T^0})c_{R^0} \qquad (5a)$$

saturation of the A site n_A is obtained from eq 3c. The use

$$n_A(c_{T^0}) = (N - [N^2 - 4c_{TA}(c_{T^0})c_{RP}(c_{T^0})]^{1/2})/[2c_{RP}(c_{T^0})] \qquad (3c)$$

$$N = c_{TA}(c_{T^0}) + c_{RP}(c_{T^0}) + 1/K_A$$

$$c_{RP}(c_{T^0}) = n_P(c_{T^0})c_{R^0}$$

of c_{RP} rather than c_{R^0} accounts for the observation that tRNA binding to the A site only takes place at ribosomes preoccupied in the P site. The difference is small anyway, since, as shown under Results, the binding constant K_P is much larger than K_A.

Finally, correlation to the amount of tRNA bound to both P and A sites, I_{PA}, yields eq 4b, where I_{max} denotes the signal for one site at saturation. Three of the four unknown pa-

$$I_{PA}(c_{T^0}) = I_{max}[n_P(c_{T^0}) + n_A(c_{T^0})] + I_B \qquad (4b)$$

rameters in eq 4b, K_P, I_{max}, and I_B, can be obtained by computer fitting; K_A is taken from a separate titration of the A site according to the single-site model. If the signal at saturation I_{max} for both sites is the same, eq 4b can be applied directly. This holds true for the titration of, e.g., radioactively labeled N-Ac[^{14}C]Phe-$tRNA^{Phe}$, since both P and A sites exhibit the same activity in binding of tRNA (Lill et al., 1984). However, in fluorescence titrations, the quantum yields of fluorescent tRNAs bound to either site are not necessarily identical. In addition, because of singlet–singlet energy transfer between the two bound fluorophores (Paulsen et al., 1983), the total fluorescence of two simultaneously bound tRNAs is not always equal to the sum of the individual signals. Both complications have been taken into account in eq 4c by

$$I_{PA}(c_{T^0}) = I_{max}[n_P(c_{T^0}) + n_A(c_{T^0})q] + I_B \qquad (4c)$$

$$q = I^A_{max}/I_{max}$$

the introduction of a correction factor q, which represents the relative saturation signal of the tRNA bound subsequently. q is obtained from a stoichiometric titration ($c_{R^0} \gg 1/K$) of both sites with fluorescent tRNA. I_{max} is read from the difference of the signals at a tRNA/ribosome ratio of 1 and 0; I^A_{max} is represented by the signal remaining up to the titration plateau.

Three-Site Model. The reaction scheme for the sequential binding of tRNA to the three ribosomal binding sites, P, A, and E, is depicted in eq 2b. The formalism of the three-site

$$R + T \underset{K_P}{\rightleftharpoons} RT_P \overset{+T}{\underset{K_A}{\rightleftharpoons}} RT_PT_A \overset{+T}{\underset{K_E}{\rightleftharpoons}} RT_PT_AT_E \qquad (2b)$$

model can be treated closely to that of the two-site model, if, in addition, subsequent binding to the third (E) site (right part of eq 2b) is considered. Thus, eq 3b, 5a, and 3c can be adopted from the last section and the fractional saturation of the E site, n_E derived according to n_A (cf. eq 5a and 3c):

$$c_{TE}(c_{T^0}) = c_{T^0} - [n_P(c_{T^0}) + n_A(c_{T^0})]c_{R^0} \qquad (5b)$$

$$n_E(c_{T^0}) = (P - [P^2 - 4c_{TE}(c_{T^0})c_{RA}(c_{T^0})]^{1/2})/[2c_{RA}(c_{T^0})] \qquad (3d)$$

$$P = c_{TE}(c_{T^0}) + c_{RA}(c_{T^0}) + 1/K_E$$

$$c_{RA}(c_{T^0}) = n_A(c_{T^0})c_{R^0}$$

Furthermore, in analogy to eq 4c, the total signal I_{PAE} is expressed by eq 4d, where q_1 and q_2, in analogy to q, denote

$$I_{PAE}(c_{T^0}) = I_{max}[n_P(c_{T^0}) + n_A(c_{T^0})q_1 + n_E(c_{T^0})q_2] + I_B \qquad (4d)$$

$$q_1 = I^A_{max}/I_{max} \qquad q_2 = I^E_{max}/I_{max}$$

the correction factors for the signal of binding to the A and E sites, respectively, relative to the P site. The parameters K_P, I_{max}, and I_B are obtained by the fitting procedure with K_A and K_E known from separation titrations. The correction factors q_1 and q_2 are determined by reading I_{max}, I^A_{max}, and I^E_{max} from a stoichiometric titration of all three binding sites, as described above for the two-site model.

Results

The existence of two and three binding sites on *E. coli* ribosomes for charged and uncharged $tRNA^{Phe}$, respectively, complicates the determination of site-specific binding constants. Since the affinities of the sites differ by factors of at least 10, the simultaneous determination of all binding constants from

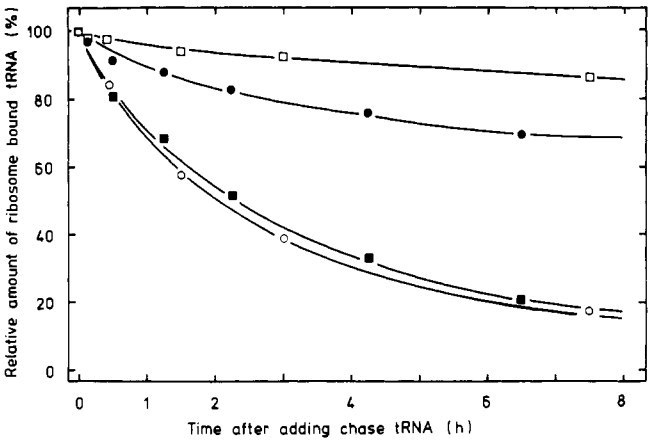

FIGURE 1: Stability of tRNA binding to the ribosomal P and A sites. P site complexes (□, ■) were formed by incubation of either [^{32}P]-tRNA^{Phe} (open symbols) or *N*-Ac[^{14}C]Phe-tRNA^{Phe} from yeast (closed symbols, 1.4 × 10^{-8} M) with poly(U)-programmed ribosomes (2.0 × 10^{-8} M) in buffer A at 20 mM Mg^{2+}; for the formation of the A site complexes (○, ●), labeled tRNAs (1.4 × 10^{-7} M), were incubated with poly(U)-programmed ribosomes (2.0 × 10^{-7} M), which were preloaded with unlabeled deacylated tRNA^{Phe} (2.5 × 10^{-7} M). Then, a 10-fold excess of unlabeled deacylated tRNA^{Phe} from yeast was added and the remaining ribosome-bound, labeled tRNA determined by the filtration assay at the times indicated. The ordinate values are given relative to the amount of bound tRNA before adding the chasing tRNA. For experimental details, see Materials and Methods.

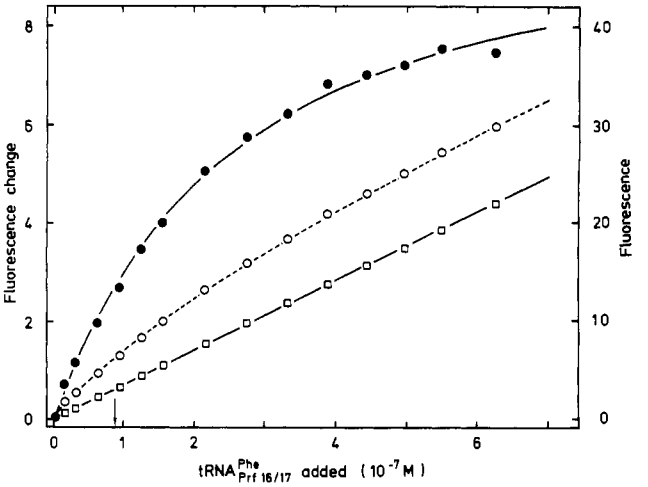

FIGURE 2: Fluorescence titration of the E site with tRNA$^{Phe}_{Prf16/17}$ from yeast in buffer A at 20 mM Mg^{2+}. After the P and A sites of poly(U)-programmed ribosomes (final concentration 9.0 × 10^{-8} M; arrow) were blocked with *N*-AcPhe-tRNA^{Phe} from yeast (see Materials and Methods), increasing amounts of fluorescent tRNA were added, and the respective fluorescence signal (○) was monitored ("complex titration"). The corresponding fluorescence data measured during a titration in omission of ribosomes (□, "reference titration") were corrected by linear regression and then subtracted from the respective complex titration data to give the final titration curve (●). In order to reveal the binding constant of the E site, the single-site model (as detailed under Materials and Methods) was fitted to the titration data. Solid lines represent the computer fits. Fluorescence was normalized such that 10 units represents the final titration plateau, i.e., saturation of the E site, which was also estimated by the computer fitting procedure.

a single titration is impractical for technical reasons. In order to determine all binding constants with comparable precision, the problem was broken down biochemically. As discussed under Materials and Methods, this approach takes advantage of the facts (i) that the ribosomal tRNA binding sites are occupied in a sequential rather than a random fashion (Watanabe, 1972; Lill et al., 1984) and that (ii) the tRNA dissociation out of the P and A sites is slow enough to be considered irreversible on the time scale of the titration experiments (the latter point is documented below). Thus, it is possible to titrate the weaker sites separately after the stronger sites have been blocked by a preincubation with stoichiometric amounts of tRNA. For instance, A site binding of charged tRNA can be studied after blocking the P site, or else E site binding of deacylated tRNA after blocking both P and A sites. In this way, the binding constants of the weaker sites are obtained separately and can subsequently be used as known parameters in the evaluation of the binding constants of the stronger sites.

Stability of tRNA–Ribosome Complexes. The use of ribosomes whose P and/or A sites are blocked to titrate the weaker sites of course requires that there is no significant exchange of the tRNA from the preoccupied sites against tRNA added during the subsequent titration. This is the case for both deacylated [^{32}P]tRNA^{Phe} and *N*-Ac[^{14}C]Phe-tRNA^{Phe} bound to either the P or to the A site of poly(U)-programmed ribosomes. As shown by chase experiments (Figure 1), both tRNA species dissociate rather slowly from the two binding sites. For deacylated tRNA^{Phe}, the half-times of dissociation range from more than 10 h (P site) to 2 h (A site) at both 20 mM (Buffer A, Figure 1) and 10 mM Mg^{2+} (buffer B, not shown). For *N*-AcPhe-tRNA^{Phe} at 20 mM Mg^{2+}, nearly the reversed situation is observed with half-times of about 2 and 10 h for P and A sites, respectively (Figure 1). At 10 mM Mg^{2+} (buffer B), the dissociation rates of *N*-AcPhe-tRNA^{Phe} from both P and A sites become quite similar with half-times around 10 h (not shown).

E Site Binding of Deacylated tRNA^{Phe}. Due to the rather high lability of the E site complexes (Lill et al., 1984), binding to the E site had to be measured by fluorescence in order to obtain reliable results. During formation of the complex, the fluorescence of the proflavin derivative of tRNA^{Phe} from yeast, tRNA$^{Phe}_{Prf16/17}$, increases by about 40%. An example for a titration experiment utilizing this effect is shown in Figure 2. Poly(U)-programmed ribosomes were preincubated with a 2.3-fold excess of *N*-AcPhe-tRNA^{Phe} from yeast to block both P and A sites and then titrated with tRNA$^{Phe}_{Prf16/17}$. In parallel, a titration was performed in the absence of ribosomes. The signal change due to complex formation was calculated as the difference between the complex and the refernece titrations (Figure 2). Analogous titrations were performed with proflavin-labeled tRNA^{Phe} from *E. coli*, tRNA$^{Phe}_{Prf16/20}$ (not shown), which exhibited a fluorescence increase of 50% upon binding to the E site. The titration curves were evaluated by using the single-site model (see Materials and Methods). Table I summarizes the association constants obtained at various ionic conditions.

Table I: Association Constants for Binding of Deacylated tRNA^{Phe} from *E. coli* and Yeast to Poly(U)-Programmed Ribosomes from *E. coli*[a]

buffer (mM Mg^{2+})	P site ($\times 10^8$ M^{-1})	A site ($\times 10^7$ M^{-1})	E site	
			E. coli ($\times 10^6$ M^{-1})	yeast ($\times 10^6$ M^{-1})
A (20)	1.8[b,c]	1.5[b–e]	28[c]	3.5[c]
C (20)	7.0[c]	8.0[b–d]	43[c]	5.0[c]
A (10)		0.17[b,d]	3.5[c]	0.9[c]
B (10)	1.4[b,c]	0.5[b,e]	5.0[c]	1.3[c]

[a] Each figure was measured at least 3 times at different ribosome concentrations; the error (SD) was estimated to be below ±25%. The extent of complex formation was determined by various methods. [b] Filtration technique employed. [c] Proflavin fluorescence employed. [d] Wybutine fluorescence employed. [e] Indicator titration assay employed.

Under all conditions, the homologous tRNA is bound to the

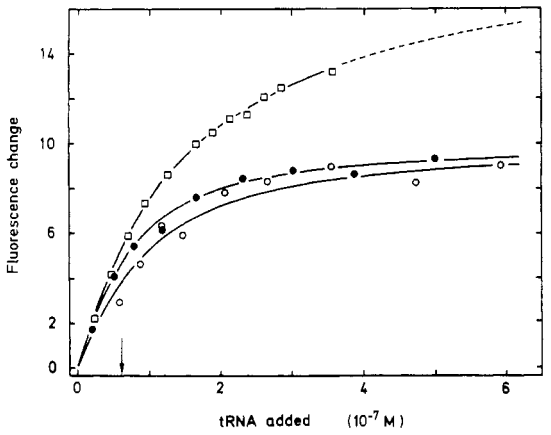

FIGURE 3: Fluorescence titrations of the A site in buffer A at 20 mM Mg^{2+} with the fluorescence emission of either proflavin ($tRNA^{Phe}_{Prf16/17}$, □) or wybutine (○, ●). P site blocked, poly(U)-programmed ribosomes (6.2×10^{-8} M, arrow) were titrated with either deacylated $tRNA^{Phe}$ (open symbols) or *N*-AcPhe-$tRNA^{Phe}$ (closed symbols) as described under Materials and Methods; the titration curves were obtained as illustrated in Figure 2. Ordinate values are normalized for the total occupancy of the A site alone. Since subsequent binding of deacylated $tRNA^{Phe}$ to the E site is only reported by the proflavin and not by the wybutine label, the titration curves using the latter were evaluated by fitting the single-site model to the titration data. For the titration of deacylated $tRNA^{Phe}_{Prf16/17}$, the two-site model was applied, which considers subsequent E site binding (see Materials and Methods). Subsequent binding of deacylated $tRNA^{Phe}_{Prf16/17}$ to the E site may be inferred from the difference of the two titration curves of deacylated $tRNA^{Phe}$.

E site stronger than the heterologous one. For instance, at 20 mM Mg^{2+}, a nearly 10-fold difference is observed, while at 10 mM Mg^{2+} the affinities differ by a factor of about 4. Table I also shows that E site binding of the two $tRNA^{Phe}$ species is insensitive to changes in the concentration of monovalent salt. Both the insensitivity to changes of the ionic strength and the low stability against dissociation are characteristic features of tRNA binding to the E site, distinguishing it from binding to both P and A sites.

A Site Binding of $tRNA^{Phe}$ and N-AcPhe-$tRNA^{Phe}$. In order to define the appropriate conditions for studying A-site binding, the time course of A site complex formation has been measured for deacylated $tRNA^{Phe}$ and N-AcPhe-$tRNA^{Phe}$ at various Mg^{2+} concentrations. Fluorescent and radioactive labels were used in parallel and yielded the same results. Nonenzymatic binding is rather slow and, in addition, strongly dependent upon the Mg^{2+} concentration. *N*-AcPhe-$tRNA^{Phe}$ binds about 2 times faster than deacylated $tRNA^{Phe}$, the half-times at 20 mM Mg^{2+} being about 2 and 5 min, respectively, at a ribosome concentration of 3×10^{-7} M. At lower Mg^{2+} concentrations, binding is even slower and, at 10 mM Mg^{2+}, requires an hour to reach completion (data not shown). During the titrations of the A site, the different rates of complex formation were accounted for by incubating the reaction mixtures for at least five half-times.

The binding of deacylated $tRNA^{Phe}$ and *N*-AcPhe-$tRNA^{Phe}$ from yeast to the A site can be monitored by the fluorescence of both proflavin in the D loop ($tRNA^{Phe}_{Prf16/17}$; Robertson & Wintermeyer, 1981) and the natural fluorophore wybutine in the anticodon loop (Paulsen et al., 1982). The low quantum yield of wybutine is not limiting here, since the relatively weak nonenzymatic binding to the A site has to be studied at rather high ribosome concentrations ($c_{R^0} \approx 1/K$; Winkler-Oswatitsch & Eigen, 1979).

Figure 3 provides some examples for fluorescence titrations, in which A site binding of deacylated $tRNA^{Phe}$ and of *N*-AcPhe-$tRNA^{Phe}$ is compared. Since *N*-AcPhe-$tRNA^{Phe}$ can

Table II: Association Constants for Binding of Charged $tRNA^{Phe}$ from *E. coli* or Yeast to Poly(U)-Programmed Ribosomes from *E. coli*[a]

buffer (mM Mg^{2+})	*N*-AcPhe-$tRNA^{Phe}$ P site ($\times 10^9$ M^{-1})	*N*-AcPhe-$tRNA^{Phe}$ A site ($\times 10^7$ M^{-1})	Phe-$tRNA^{Phe}$ A site ($\times 10^7$ M^{-1})
A (20	0.6[b]	3.0[b-d]	20[b]
C (20)	3.0[b]	6.0[b,c]	100[b]
A (10)	1.1[b]	0.74[b,d]	1.0[b]
B (10)	5.0[b]	2.2[b,d]	2.0[b]
B (6)	0.8[b]	<0.2[b]	

[a] Each figure was measured at least 3 times at different ribosome concentrations; the error (SD) was estimated to be below ±25%. The association constants for binding the ternary complex Phe-$tRNA^{Phe}$·EF-Tu·GTP to the A site were found to be larger than 10^{11} M^{-1}, at any condition listed. For further details see text. The extent of complex formation was determined by various methods. [b] Filtration technique employed. [c] Wybutine fluorescence employed. [d] Indicator titration assay employed.

only bind to the A site of the P site blocked ribosomes, the corresponding titration curve was evaluated by using the single-site model (see Materials and Methods). Deacylated $tRNA^{Phe}$ from yeast, however, also binds to the E site after the A site is occupied. It is important to note, though, that the fluorescence of wybutine is not affected by E site binding; hence, this type of titration can also be evaluated by using the single-site model without the need of any correction. On the other hand, as shown above, the proflavin label does report the binding of $tRNA^{Phe}_{Prf16/17}$ to the E site, thus leading to the characteristic titration curve depicted in Figure 3. For the evaluation of this curve in terms of A site binding, the additional fluorescence change has to be regarded for by applying the two-site model, making use of the known binding constant of the E site. The correction factor q, which is necessary to account for the different quantum yields of fluorescent tRNA bound to either site, was taken from stoichiometric titrations of both sites as $q = 1.0 \pm 0.1$ (for details, see Materials and Methods). As evident from Figure 3 and demonstrated for a variety of ionic conditions (see Table I), the two approaches used for the titrations with deacylated $tRNA^{Phe}$ yield identical results; i.e., the introduction of the proflavin label into the tRNA does not influence its A site binding properties.

As demonstrated above, the A site forms a stable complex with $tRNA^{Phe}$. Therefore, the extent of complex formation can also be measured by nitrocellulose filtration, although, in principle, this assay represents a nonequilibrium method. The titrations performed with the radioactively labeled [^{32}P]-$tRNA^{Phe}$ and *N*-Ac[^{14}C]Phe-$tRNA^{Phe}$ from both *E. coli* and yeast confirm the results obtained by the fluorescence technique (Tables I and II).

The binding constants of the A site were also determined by an indirect two-step indicator titration (Lill et al., 1984). In this assay ribosomes are first incubated with increasing amounts of the tRNA under study. Then, the fraction of unoccupied A sites is determined by the availability for subsequently added ternary complex [^{14}C]Phe-$tRNA^{Phe}$·EF-Tu·GTP ("indicator"), which specifically binds to the A site. This method allows one to study the binding of unlabeled tRNA. The assay has been used to follow the A site titrations with deacylated $tRNA^{Phe}$ and *N*-AcPhe-$tRNA^{Phe}$ from both *E. coli* and yeast; examples are shown in Figure 4. Differences in the binding strength are indicated by the steepness of the sigmoidal curves. The quantitative evaluation of the binding constants was done by fitting a binding model to the data (Lill et al., 1984). Identical results as compared to the other two methods are obtained (Tables I and II).

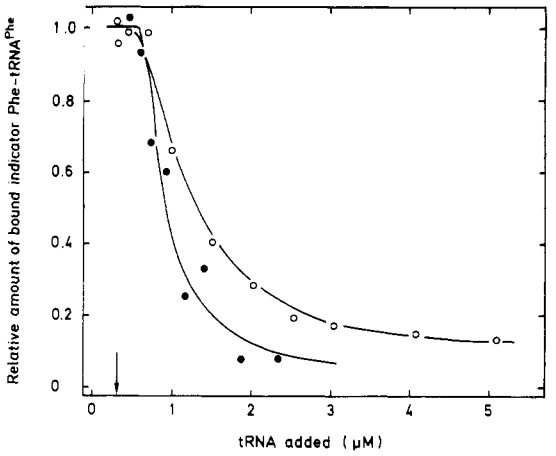

FIGURE 4: Indicator titration of the A site. P site blocked ribosomes (3×10^{-7} M, arrow) were titrated with *N*-Ac[^{14}C]Phe-tRNA^{Phe} of low specific radioactivity (closed symbols) or deacylated tRNA^{Phe} (open symbols) in buffer B at 10 mM Mg^{2+} and incubated for 90 min. Then, ternary complex [^{14}C]Phe-tRNA^{Phe}·EF-Tu·GTP of high specific radioactivity (final concentration 1×10^{-7} M) was added and the bound Phe-tRNA^{Phe} isolated by the filtration assay after an incubation of 30 s. The titration curves were analyzed by a computer fitting procedure applying the binding model described by Lill et al. (1984); the solid lines represent the computer fits.

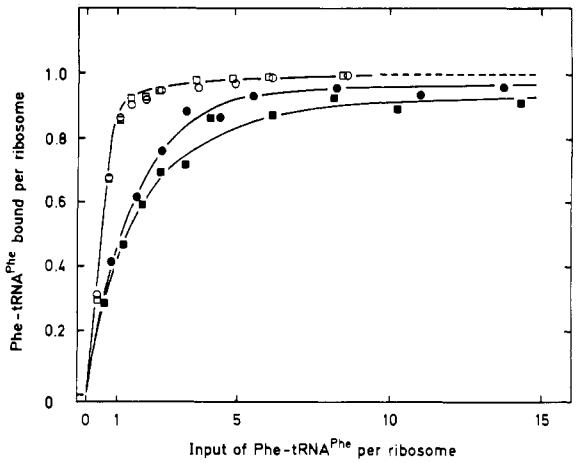

FIGURE 5: Influence of elongation factor Tu and GTP upon the affinity of binding Phe-tRNA^{Phe} to the A site. The titrations of P site blocked poly(U)-programmed ribosomes with [^{14}C]Phe-tRNA^{Phe} were performed in the absence (closed symbols) or presence (open symbols) of EF-Tu·GTP in buffer A (20 mM Mg^{2+}; ○, ●) and buffer B (10 mM Mg^{2+}; □, ■) as described under Materials and Methods. Complex formation was followed by the filtration technique and data evaluation performed by using the single-site model (see Materials and Methods). Ribosome concentrations in the absence of EF-Tu were 1×10^{-8} (buffer A) and 6×10^{-8} M (buffer B); in the presence of EF-Tu, it was kept at 6.7×10^{-10} M for both ionic conditions.

From the summary of the binding constants in Tables I and II, it is evident that *N*-AcPhe-tRNA^{Phe} and deacylated tRNA^{Phe} behave quite similarly at 20 mM Mg^{2+}, while at 10 mM Mg^{2+} the former binds to the A site about 4 times stronger than the latter (see also Figures 3 and 4). The affinity of both tRNA species is affected in a similar fashion by changes of the ionic conditions. The reciprocal effect of Mg^{2+} and monovalent ions is clearly reflected in the binding constants: they are reduced by either lowering the concentration of Mg^{2+} or increasing the concentration of monovalent ions.

A Site Binding of Phe-tRNA^{Phe}. In order to compare the affinities under nonenzymatic and enzymatic conditions, A site binding of [^{14}C]Phe-tRNA^{Phe} and the ternary complex [^{14}C]Phe-tRNA^{Phe}·EF-Tu·GTP was studied (Figure 5). Nonenzymatic binding was performed in the presence of phenylalanyl-tRNA ligase, [^{14}C]phenylalanine, and ATP ("in situ aminoacylation"), in order to keep the charging level of the tRNA high during the time needed for A site binding.

The results summarized in Table II show that there is no particular preference of the A site for Phe-tRNA^{Phe}, as compared to *N*-AcPhe-tRNA^{Phe}. At 10 mM Mg^{2+}, essentially the same binding constant were found for the two charged tRNAs. Only at 20 mM Mg^{2+} an about 10-fold higher binding strength of Phe-tRNA^{Phe} was observed. As compared with deacylated tRNA^{Phe}, the affinity differences are somewhat more pronounced (Table I), its binding to the A site being weaker by factors between 4 and 10, depending on the ionic conditions.

Binding of Phe-tRNA^{Phe} in the presence of EF-Tu·GTP was found to be very strong. As evident from Figure 5, no significant deviation from a stoichiometric uptake of the ternary complex was observed, even at very low ribosome concentrations. From the evaluation of the titrations at the lowest ribosome concentration examined (1×10^{-10} M), apparent binding constants of greater than 10^{11} M^{-1} are estimated (Table II). It should be stressed that this affinity increase by a factor of 10^4 as compared to Phe-tRNA^{Phe} alone is not due to a higher affinity of the ternary complex itself, since the figure includes the energy of GTP hydrolysis, which is coupled, at least partially, to the binding reaction. Therefore, the high occupancy of the A site, which, due to the extremely slow dissociation of Phe-tRNA^{Phe}, prevails after the dissociation of EF-Tu·GDP, does not represent a true equilibrium situation.

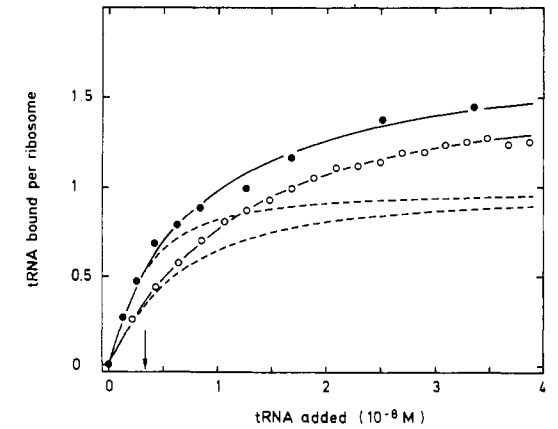

FIGURE 6: Equilibrium titrations of the ribosomal P site as monitored by both the fluorescence and the filtration techniques. Poly(U)-programmed ribosomes (3×10^{-9} M, arrow) were titrated with increasing amounts of either *N*-Ac[^{14}C]Phe-tRNA^{Phe} (●) or deacylated tRNA$^{Phe}_{Prf16/17}$ (○) in buffer A at 20 mM Mg^{2+} as described under Materials and Methods. After incubation for 30 min, the extent of complex formation was analyzed by the filtration assay or by the procedure detailed in Figure 2. In order to consider subsequent binding to the A and A plus E sites, the evaluation of the binding parameters was performed by using the two- or three-site model (see Materials and Methods), respectively. These parameters were used to calculate fractional saturation of the P site alone (broken lines).

P Site Binding of tRNA^{Phe} and N-AcPhe-tRNA^{Phe}. The P site of poly(U)-programmed ribosomes is the first site to be occupied. For evaluating the titration curves, subsequent binding to the A and E sites was calculated on the basis of the binding constants, determined above, and included in the evaluation of P site binding (see Materials and Methods). Examples for P site titrations with tRNA$^{Phe}_{Prf16/17}$ and N-Ac-[^{14}C]Phe-tRNA^{Phe}, performed by employing the fluorescence and the filtration technique, respectively, are shown in Figure 6. The extent of subsequent binding to the A and E sites is illustrated by the differences between the observed titration curves and the respective calculated curves representing the saturation of the P site alone. In stoichiometric titrations performed separately, the correction factors q_1 and q_2, nec-

Table III: Association Constants for Binding of Deacylated $tRNA^{Phe}$ and Charged $tRNA^{Phe}$ from *E. coli* and Yeast to Nonprogrammed Ribosomes from *E. coli*[a]

buffer (mM Mg^{2+})	deacylated $tRNA^{Phe}$					*N*-AcPhe-$tRNA^{Phe}$
	stoichiometric determination			E site specific determination		
	K_1	K_2 (yeast)	K^b	*E. coli*	yeast	P site
A (20)	5.0[c]	1.6[c]	2.8[c]	7.5[c]	2.5[c]	6.0[d,e]
C (20)	11.0[c]	3.0[c]	5.7[c]		3.0[c]	13.0[d,e]
B (15)	2.8[c]	0.85[c]	1.5[c]		1.2[c]	
B (10)						0.7[d,e]

[a] All figures are given in units of 10^6 M^{-1}. Each figure was measured at least 3 times at different ribosome concentrations; the error (SD) was estimated to be below ±40%. [b] Site-specific binding constant for both P and E sites. The figures were assessed from K_1 and K_2 by the assumption of identical, noninteracting binding constants. For further details see text. The extent of complex formation was determined by various methods. [c] Proflavin fluorescence employed. [d] Wybutine fluorescence employed. [e] Filtration technique employed.

essary for the consideration of the different fluorescence contributions of A and E site bound $tRNA^{Phe}_{Prf16/17}$, respectively, were determined to be 0.9 ± 0.1 and 1.4 ± 0.2 (for details, see Materials and Methods).

The results of P site titrations with deacylated $tRNA^{Phe}$ and *N*-AcPhe-$tRNA^{Phe}$ at different ionic conditions are summarized in Tables I and II. The affinity of the P site for N-AcPhe-$tRNA^{Phe}$ generally is stronger by at least a factor of 4. The binding strength of *N*-AcPhe-$tRNA^{Phe}$ increases, rather than decreases, upon lowering the Mg^{2+} concentration from 20 to 10 mM. Such a behavior appears to be a peculiarity of the P site interaction of this tRNA species, since the opposite effect is observed for P site binding of deacylated $tRNA^{Phe}$ and, likewise, for the binding to the other two ribosomal sites (see above). On the other hand, upon lowering the concentration of monovalent salt, a stronger binding is observed for all three tRNA species.

In order to assess more closely the influence of the ionic strength upon the affinity of tRNA binding to the P site, salt titrations were performed at fixed concentrations of tRNA and ribosomes. A change in the binding affinity is expected to show up in a different extent of complex formation; the maximum effect is obtained when the concentrations of the complex partners match the dissociation constant of the complex at an intermediate salt concentration. As an example, Figure 7 shows the influence of the NH_4Cl concentration on the binding of both *N*-AcPhe-$tRNA^{Phe}$ and $tRNA^{Phe}_{Prf16/17}$ at 10 mM Mg^{2+}, as measured by the filtration and the fluorescence technique, respectively. Bell-shaped curves are obtained for both tRNA species; maximum binding is found at 25 mM NH_4Cl. Similar curves are observed at 20 mM Mg^{2+}, the maximum being shifted to somewhat higher ionic strength, 35 mM NH_4Cl (not shown). This behavior clearly demonstrates the competition of monovalent cations with magnesium ions, the latter stabilizing the complex.

From the data of Figure 7, the number of ionic interactions involved in binding to the P site can be estimated, if it is assumed that no anions are displaced during complex formation (Record et al., 1976, 1978). Following this treatment, which involves a plot of log K_a vs. $-\log c_{M^+}$ (Figure 7, inset), values of 2.1 or 2.6 ion pairs are obtained for deacylated $tRNA^{Phe}_{Prf16/17}$, assuming the exclusive binding of either double- or single-stranded regions of the tRNA, respectively (Record et al., 1978). For *N*-AcPhe-$tRNA^{Phe}$, the respective numbers are 4.7 and 6.0 ion pairs. Hence, about three and five ion pairs are formed during P site binding of deacylated $tRNA^{Phe}_{Prf16/17}$ and *N*-AcPhe-$tRNA^{Phe}$, respectively. However, the major part of the binding energy is contributed by nonionic interactions, corresponding to binding constants of 10^6 and 10^5 M^{-1}, respectively.

tRNA Binding to Nonprogrammed Ribosomes. In the absence of mRNA, *E. coli* ribosomes exhibit only one binding site for *N*-AcPhe-$tRNA^{Phe}$, the P site, and two binding sites for deacylated $tRNA^{Phe}$, and P and E sites (Grajevskaja et al., 1982; Kirillov et al., 1983; Lill et al., 1984). Binding to the A site is not detectable in the absence of mRNA. Even for the ternary complex Phe-$tRNA^{Phe}$·EF-Tu·GTP, no significant A site complex formation is observable as judged from both filtration and fluorescence experiments (data not shown). Therefore, at any condition used here and for all tRNA species examined, binding to the noncoded A site must be weaker than 10^5 M^{-1}. A similar result has been obtained for the interaction of the poly(U)-programmed A site with the near-cognate ternary complex containing Leu-$tRNA^{Leu}_2$ (Thompson & Karim, 1982).

The affinities for the binding of *N*-AcPhe-$tRNA^{Phe}$ to the P site of nonprogrammed ribosomes were determined by using the filtration assay and by measuring wybutine fluorescence (not shown). The P site location was verified by the puromycin reactivity of the bound material. The titrations were evaluated by employing the single-site model, since there is no further binding to other sites (Table III). Compared to the affinity found for the poly(U)-programmed P site, the binding strength

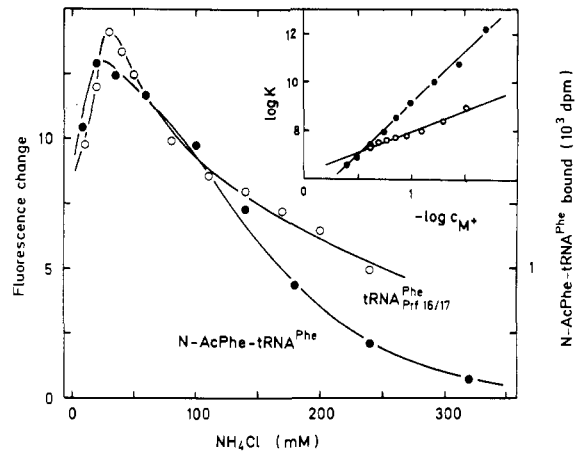

FIGURE 7: Dependence of the P site affinity upon the concentration of monovalent salt. Either *N*-Ac[^{14}C]Phe-$tRNA^{Phe}$ or $tRNA^{Phe}_{Prf16/17}$ (1×10^{-8} M) was incubated with poly(U)-programmed ribosomes (1×10^{-8} M) in 10 mM Tris-HCl, pH 7.5, 10 mM magnesium acetate, 1 mM dithioerythritol, and NH_4Cl as indicated at 20 °C for 30 min in separate reaction mixtures. Complex formation was measured by either the filtration technique or the fluorescence assay; for each point, the respective blank values measured in the absence of ribosomes were subtracted. For the assessment of the number of ionic interactions involved in tRNA binding to the P site, data were plotted (insert) according to Record et al. (1976). Maximum binding essential for the calculation of the log *K* values was taken either from the fluorescence measured in the presence of a 5-fold excess of ribosomes or from the input of *N*-Ac[^{14}C]Phe-$tRNA^{Phe}$ as determined by TCA precipitation.

is reduced by 2–4 orders of magnitude depending upon Mg^{2+} concentration.

A more complicated situation is encountered with deacylated $tRNA^{Phe}$, since due to the substantial reduction of the stability of the P site complex, which is caused by the omission of poly(U), $tRNA^{Phe}$ no longer binds to P and E sites in a sequential fashion. Nevertheless, it was possible to block the P site by the addition of *N*-AcPhe-$tRNA^{Phe}$ (3-fold excess) and to titrate the E site specifically with either yeast $tRNA^{Phe}_{Prf16/17}$ or *E. coli* $tRNA^{Phe}_{Prf16/20}$ (data not shown). The binding constants obtained for various ionic conditions are summarized in Table III.

The random occupancy of P and E sites with deacylated $tRNA^{Phe}$ precludes the separate determination of the P site affinity. In the absence of additional information, only stoichiometric ("macroscopic") rather than site-specific ("microscopic") binding constants can be determined from simultaneous titration of both P and E sites (Klotz, 1974; Klotz & Hunston, 1975). The titrations were performed with the fluorescent $tRNA^{Phe}$ derivatives (data not shown) and were evaluated by fitting an equation for two binding sites given by Klotz and Hunston (1975). The resulting binding constants K_1 and K_2, summarized in Table III, differ by factors of about 3 for all ionic conditions examined. Since the stoichiometric binding constants of two identical, noninteracting binding sites differ by a factor of 4, just for statistical reasons (Klotz & Hunston, 1979; Cantor & Schimmel, 1980), the observed difference indicates rather similar site-specific binding constants for P and E sites and little, if any, interaction between the two sites. With this assumption, K_1 and K_2 served to assess the site-specific binding constants, K, for both P and E sites. As seen from Table III, the two approaches, i.e., the stoichiometric and the site-specific determination, yield consistent results.

As found for *N*-AcPhe-$tRNA^{Phe}$, binding of deacylated $tRNA^{Phe}$ to the noncoded P site is weaker by at least 2 orders of magnitude as compared to the presence of poly(U) (cf. Tables I and III) and is found to be weaker than 10^5 M^{-1} at 10 mm Mg^{2+} and below. This rather strong influence of codon–anticodon interaction for binding to the P site confirms qualitative results reported earlier (Robertson et al., 1977; Lührmann et al., 1979; Wurmbach & Nierhaus, 1979; Peters & Yarus, 1979). The affinity of the E site, on the other hand, is not appreciably influenced by the presence or absence of the mRNA. The data given in Tables I and III show that for $tRNA^{Phe}$ from yeast the binding constants for the E site are identical in both cases; for $tRNA^{Phe}$ from *E. coli*, poly(U) only slightly (4-fold) increases the binding constant of the E site.

Discussion

Affinities of P and A Sites. Most of the previous reports agree in showing that both deacylated $tRNA^{Phe}$ and *N*-AcPhe-$tRNA^{Phe}$ are bound 10–50 times more strongly to the P site than to the A site of poly(U)-programmed *E. coli* ribosomes. Our present data, which have been obtained at a variety of conditions with respect to Mg^{2+} concentration and ionic strength, are consistent with this general result (Tables I and II). It should be noted, though, that at 10 mM Mg^{2+} concentration the preference of the P site over the A site is even higher, about 200-fold. As discussed below, this observation may be relevant for the mechanism of translocation, since at this condition the elongation rate of our system in vitro is about five phenylalanines ribosomes^{-1} s^{-1} (at 20 °C), which is close to maximal.

While for *N*-AcPhe-$tRNA^{Phe}$ our binding constants are in good agreement with the ones obtained by Kirillov and Semenkov (1982) for deacylated $tRNA^{Phe}$, these authors reported a 10–100-fold stronger P site binding (Kirillov et al., 1983). To us, the main reason for the discrepancy seems to be that these authors, to avoid the problem of A and E site occupancy, titrated tRNA by adding ribosomes in excess. We observed that, by using this technique, the occupation of the P site may be overestimated. On the other hand, the rather low affinity reported by Rheinberger et al. (1981) probably is due to the fact that it was determined from a stoichiometric titration.

Aminoacylation of $tRNA^{Phe}$ generally increases the binding strength, as evident from the comparison of the binding constants of $tRNA^{Phe}$ with that of Phe-$tRNA^{Phe}$ in the A site (about 10-fold increase) or *N*-AcPhe-$tRNA^{Phe}$ in the P site (40-fold increase at 10 mM Mg^{2+}; Tables I and II). However, from our data on nonenzymatic A site binding of Phe-$tRNA^{Phe}$ there is no indication for the very high affinity binding, 10^{11} M^{-1}, reported by Kirillov et al. (1978).

It is known that both the rate and the extent of aminoacyl-tRNA binding to the A site are increased considerably by the addition of elongation factor Tu and GTP. However, the effects of stimulation of the binding step due to ternary complex formation and of increasing the binding efficiency by coupling the reaction to GTP hydrolysis have not yet been sorted out quantitatively. Working with GTP(γS), a GTP analogue that is hydrolyzed very slowly, Thompson and Karim (1982) determined, by kinetic measurements, a binding constant for the ternary complex of about 10^9 M^{-1}. Thus, as compared to Phe-$tRNA^{Phe}$ alone (Table II), the binding constant is increased about 100-fold by the presence of EF-Tu·GTP(γS). In the physiological reaction, the hydrolysis of GTP provides the energy for the, thermodynamically unfavorable, removal of EF-Tu, which is necessary for the elongation to continue, thereby increasing the efficiency of the process. This, in addition to proofreading (Kurland & Ehrenberg, 1984), probably is the main function of GTP hydrolysis during aminoacyl tRNA binding to the A site.

tRNA Binding Properties of the E Site. The E site differs from both P and A sites in a number of important properties, including the specificity for deacylated tRNA (Rheinberger et al., 1981; Grajevskaja et al., 1982; Kirillov et al., 1983; Lill et al., 1984), as well as the low stability and the lack of mRNA dependence of tRNA binding (Grajevskaya et al., 1982; Kirillov et al., 1983; Lill et al., 1984). The latter results are at variance with the stable, mRNA-dependent E site binding of $tRNA^{Phe}$ reported by Rheinberger et al. (1981). However, mRNA-independent binding to the E site is also supported by the finding that several noncognate tRNAs efficiently compete with $tRNA^{Phe}$ for binding to the E site of poly(U)-programmed ribosomes (Wintermeyer et al., 1986). According to the present quantitative data, the affinity of the E site for binding *E. coli* $tRNA^{Phe}$ is lowered only slightly (4-fold) by the omission of poly(U). Hence, codon–anticodon interaction does not contribute appreciably to the binding of tRNA in the E site.

It has been proposed that during translocation the E site functions as an exit site where the deacylated tRNA, after being released from the P site, is bound in a codon-dependent manner (Rheinberger & Nierhaus, 1983; Nierhaus & Rheinberger, 1984). On the basis of the premise that codon–anticodon interaction of only the P site bound tRNA is insufficiently strong to keep the mRNA in a fixed position on the ribosome, these authors have postulated that the interaction of E site bound tRNA with the mRNA is important in order to prevent slippage of the mRNA after translocation. However, the properties of the E site, discussed above, do not

support this proposal, simply because in the E site the tRNA is bound weakly and does not efficiently interact with the mRNA. Moreover, in view of the extremely high stability of the P site complexes of $tRNA^{Phe}$ and N-AcPhe-$tRNA^{Phe}$, there is no a priori reason to postulate the necessity of an additional codon–anticodon interaction.

Functional Role of an Exit Site in Translocation. It has been suggested (Leder, 1973; Holschuh et al., 1981) that the translocation proceeds in two steps, the EF-G- and GTP-dependent release of the deacylated tRNA from the P site and the subsequent displacement of the peptidyl tRNA. The latter step was thought to occur spontaneously, being driven by the free energy gained by displacing the peptidyl-tRNA from the lower affinity A site to the higher affinity P site, which, according to the present data, amounts to about −3 kcal/mol. [Here and in the following, standard free energies are used, which are calculated from the equilibrium constants obtained in buffer B (10 mM Mg^{2+}), Tables I and II.] However, these models do not explain the fact that the displacement of peptidyl-tRNA from the A site to the P site proceeds efficiently, albeit slowly, in the absence of EF-G and GTP ("spontaneous translocation"; Bergemann & Nierhaus, 1983) or, at a high rate, in the presence of EF-G and nonhydrolyzable GTP analogues (Inoue-Yokosawa et al., 1974; Modolell et al., 1975), i.e., that the reaction is exergonic to a large extent also without the hydrolysis of GTP. Without GTP hydrolysis, the loss of free energy due to the dissociation of the deacylated tRNA from the P site renders the translocation reaction thermodynamically extremely unfavorable, the free energy being about 8 kcal/mol. The problem is eliminated by the availability of an additional site, the E site, where the deacylated tRNA is bound after leaving the P site. On the basis of such a three-site model, the synchronous displacement of the two tRNAs is exergonic by about 1 kcal/mol, as calculated from the difference in the free energies of P site binding of *N*-AcPhe-$tRNA^{Phe}$ and of $tRNA^{Phe}$, about −2 kcal/mol, minus the free energy difference between A site binding of N-AcPhe-$tRNA^{Phe}$ and E site binding of $tRNA^{Phe}$, about −1 kcal/mol.

The thermodynamic argument, which applies for the spontaneous translocation observed with isolated ribosomal complexes, is not necessarily relevant for elongating ribosomes in vivo or under the conditions of factor-free translation (Gavrilova et al., 1976). For elongating systems, the kinetic advantage of an intermediate ribosome-bound state of the leaving tRNA appears to be more important. The activation energy required for the one-step dissociation of the tRNA from the P site is at least as high as, and probably much higher than, the free energy of P site binding, about −11 kcal/mol for $tRNA^{Phe}$. On the other hand, the minimal activation energy for the release of $tRNA^{Phe}$ from the E site equals the free energy of binding to this site, −9 kcal/mol. Even the 2 kcal/mol difference of the activation energies, which probably is much larger based upon the large stability difference of tRNA binding to the two sites (at least thousand-fold), could result in an about 30-fold higher rate of the two-step reaction as compared to the one-step reaction.

To gain the acceleration, two conditions have to be fulfilled. First, the activation energy of the tRNA displacement from the P site of the E site has to be lower than that of the one-step reaction; this is very likely, since the tRNA does not have to dissociate from the ribosome during that step. Second, it is important that the displacement of the tRNAs is driven far from equilibrium. Under in vivo conditions, this is accomplished by suppressing the backward reaction by subsequent reactions, including dissociation of EF-G after GTP hydrolysis, A site binding of aminoacylated tRNA, and aminoacylation of the released deacylated tRNA. In the cell, most of the non-ribosome-bound tRNA is aminoacylated. Hence, the specificity of the E site for deacylated tRNA effectively prevents the reentry of tRNA via this site, which otherwise might be inhibitory.

The rate of the elongation cycle in vivo is influenced, if not limited, by the rate of translocation. Thus, the advantage gained by accelerating this step will probably be significant enough to establish and conserve a mechanism of tRNA release from the P site involving the intermediate binding to an exit site, which binds the tRNA with moderate affinity. In order not to limit the rate of elongation, the subsequent dissociation of the tRNA from this site has to be fast. The E site does not fully meet this requirement, since the rate of tRNA dissociation from this site still is about 10 times lower than the elongation rate (Wintermeyer et al., 1984). In fact, there is kinetic evidence indicating that, under conditions close to physiological ones, the leaving tRNA is transiently bound in a state that is different from, but related to, the E site bound state and from which the tRNA dissociates rapidly (Paulsen & Wintermeyer, 1986; J. Robertson, unpublished). The transient occupation by the leaving tRNA of the latter state may well represent the pathway used in vivo.

Registry No. GTP, 86-01-1; Mg, 7439-95-4; poly(U), 27416-86-0.

References

Bergemann, K., & Nierhaus, K. H. (1983) *J. Biol. Chem. 258*, 15105–15113.

Cantor, C. R., & Schimmel, P. R. (1980) *Biophysical Chemistry*, Part III, Freeman, San Francisco.

Chinali, G., Wolf, H., & Parmeggiani, A. (1977) *Eur. J. Biochem. 75*, 55–65.

Fairclough, R. H., Cantor, C. R., Wintermeyer, W., & Zachau, H. G. (1979) *J. Mol. Biol. 132*, 557–573.

Gavrilova, L. P., Kostiashkina, O. E., Koteliansky, V. E., Rutkevitch, N. M., & Spirin, A. S. (1976) *J. Mol. Biol. 101*, 537–552.

Grajevskaja, R. A., Ivanov, Y. V., & Saminsky, E. M. (1982) *Eur. J. Biochem. 128*, 47–52.

Graybill, F. A. (1969) *Introduction of Matrices with Application in Statistics*, Wadworth, Belmont, CA.

Guêron, M., & Leroy, J. L. (1978) *Anal. Biochem. 91*, 691–695.

Hirsch, R., & Zachau, H. G. (1976) *Hoppe Seyler's Z. Physiol. Chem. 357*, 509–526.

Holschuh, K., Riesner, D., & Gassen, H. G. (1981) *Nature (London) 293*, 675–677.

Inoue-Yokosawa, N., Ishikawa, C., & Kaziro, Y. (1974) *J. Biol. Chem. 249*, 4321–4323.

Kirillov, S. V., & Semenkov, Y. P. (1982) *FEBS Lett. 148*, 235–238.

Kirillov, S. V., Makhno, V. I., Odinzov, V. B., & Semenkov, Y. P. (1978) *Eur. J. Biochem. 89*, 305–313.

Kirillov, S. V., Makarov, E. M., & Semenkov, Y. P. (1983) *FEBS Lett. 157*, 91–94.

Klotz, I. M. (1974) *Acc. Chem. Res. 7*, 162–168.

Klotz, I. M., & Hunston, D. L. (1975) *J. Biol. Chem. 250*, 3001–3009.

Klotz, I. M., & Hunston, D. L. (1979) *Arch. Biochem. Biophys. 193*, 314–328.

Kurland, C. G., & Ehrenberg, M. (1984) *Prog. Nucleic Acids Res. Mol. Biol. 31*, 191–219.

Leberman, R., Antonsson, B., Giovanelli, R., Guariguata, R., Schumann, R., & Wittinghofer, A. (1980) *Anal. Biochem. 104*, 29–36.

Leder, P. (1973) *Adv. Protein Chem. 27*, 213–242.
Lill, R., Robertson, J. M., & Wintermeyer, W. (1984) *Biochemistry 23*, 6710–6717.
Lührmann, R., Eckhardt, H., & Stöffler, G. (1979) *Nature (London) 280*, 423–425.
Modolell, J., Girbés, T., & Vázquez, D. (1975) *FEBS Lett. 60*, 109–113.
Nierhaus, K. H., & Rheinberger, H.-J. (1984) *Trends Biochem. Sci. (Pers. Ed.) 9*, 428–432.
Noll, H. (1966) *Science (Washington, D.C.) 151*, 1241–1245.
Paulsen, H., & Wintermeyer, W. (1986) *Biochemistry* (in press).
Paulsen, H., Robertson, J. M., & Wintermeyer, W. (1982) *Nucleic Acids Res. 10*, 2651–2663.
Paulsen, H., Robertson, J. M., & Wintermeyer, W. (1983) *J. Mol. Biol. 167*, 411–426.
Peters, M., & Yarus, M. (1979) *J. Mol. Biol. 134*, 471–491.
Record, M. T., Jr., Lohman, T. M., & deHaseth, P. L. (1976) *J. Mol. Biol. 107*, 145–158.
Record, M. T., Jr., Anderson, C. F., & Lohman, T. M. (1978) *Q. Rev. Biophys. 11*, 103–178.
Rheinberger, H.-J., & Nierhaus, K. H. (1983) *Proc. Natl. Acad. Sci. U.S.A. 80*, 4213–4217.
Rheinberger, H.-J., Sternbach, H., & Nierhaus, K. H. (1981) *Proc. Natl. Acad. Sci. U.S.A. 78*, 5310–5314.
Robertson, J. M., & Wintermeyer, W. (1981) *J. Mol. Biol. 151*, 57–79.
Robertson, J. M., Kahan, M., Wintermeyer, W., & Zachau, H. G. (1977) *Eur. J. Biochem. 72*, 117–125.
Schmitt, M., Neugebauer, U., Bergmann, C., Gassen, H. G., & Riesner, D. (1982) *Eur. J. Biochem. 127*, 525–529.
Thompson, R. C., & Karim, A. M. (1982) *Proc. Natl. Acad. Sci. U.S.A. 79*, 4922–4926.
Watanabe, S. (1972) *J. Mol. Biol. 67*, 443–457.
Wettstein, F. O., & Noll, H. (1965) *J. Mol. Biol. 11*, 35–53.
Winkler-Oswatitsch, R., & Eigen, M. (1979) *Angew. Chem. 91*, 20–51.
Wintermeyer, W., & Zachau, H. G. (1979) *Eur. J. Biochem. 98*, 465–475.
Wintermeyer, W., & Robertson, J. M. (1982) *Biochemistry 21*, 2246–2252.
Wintermeyer, W., Lill, R., Paulsen, H., & Robertson, J. M. (1984) in *Mechanisms of Protein Synthesis* (Bermek, E., Ed.) pp 76–89, Springer, Berlin and Heidelberg.
Wintermeyer, W., Lill, R., Paulsen, H., & Robertson, J. M. (1986) in *Structure, Function, and Genetics of Ribosomes* (Hardesty, B., & Kramer, G., Eds.) Springer, New York (in press).
Wurmbach, P., & Nierhaus, K. H. (1979) *Proc. Natl. Acad. Sci. U.S.A. 76*, 2143–2147.

Biosynthetic *alr* Alanine Racemase from *Salmonella typhimurium*: DNA and Protein Sequence Determination†

Nicholas G. Galakatos, Elisabeth Daub, David Botstein, and Christopher T. Walsh*

Departments of Chemistry and Biology, Massachusetts Institute of Technology, Cambridge, Massachusetts 02139

Received October 15, 1985; Revised Manuscript Received January 13, 1986

ABSTRACT: The nucleotide sequence of the *alr* gene encoding the biosynthetic alanine racemase in *Salmonella typhimurium* is reported. The sequence was determined by the dideoxy chain termination method of Sanger mostly from recombinants derived from shotgun and specific subcloning of a 2.6-kilobase region containing the *alr* gene. The final bridging of nonoverlapping contiguous sequences was accomplished with the use of synthetic site-specific primers. The *alr* gene was found to be 1077 base pairs in length encoding a protein of 359 amino acid residues. Comparison of *alr* with the *dadB* gene encoding the catabolic alanine racemase in *S. typhimurium* revealed almost identical size (1077 vs. 1068 base pairs) and 52% sequence identity. The respective gene products displayed 43% homology, which includes a decapeptide bearing the pyridoxal 5′-phosphate binding site.

A key building block in the peptidoglycan layer of bacterial cell walls is D-alanine. The biosynthetic route to D-alanine is by racemization of L-alanine. Recent studies from these laboratories (Wasserman et al., 1983) demonstrated the presence of two genes, *dadB* and *alr*, from *Salmonella typhimurium*, both encoding alanine racemases.

The *dadB* gene encodes an alanine racemase that maps adjacent to the *dadA* gene, which in turn encodes a D-alanine dehydrogenase. The *dadB* and *dadA* gene products permit *Salmonella* to grow on L-alanine as a source of carbon and nitrogen, and thus the *dadB* alanine racemase may have primarily a catabolic function. The *dadB* gene has been sequenced, the encoded alanine racemase purified to homogeneity (Wasserman et al., 1984), and its molecular basis of susceptibility to β-haloalanine antibacterials determined (Badet et al., 1984).

The second alanine racemase gene in *S. typhimurium* is *alr*, which has now been mapped to minute 91 and isolated from a λ library (E. Daub et al., unpublished results). In the accompanying paper (Esaki & Walsh, 1986), we describe the purification of the cloned *alr*-encoded alanine racemase to homogeneity, its enzymatic characteristics and susceptibility to haloalanines, and the *N*-terminal and active site protein

† Financial support from the National Science Foundation (Grant PCM 8308969) is gratefully acknowledged.

* Address correspondence to this author at the Department of Chemistry.

0006-2960/86/0425-3255$01.50/0